

# Synthesis and characterization of novel bifunctional mesoporous silica catalyst and its scope for one-pot deacetalization–knoevenagel reaction

Surjyakanta Rana · Suresh Maddila ·  
Ramakanth Pagadala · Sreekantha B. Jonnalagadda

Published online: 8 January 2015  
© Springer Science+Business Media New York 2015

**Abstract** Bifunctional (both sulfonic and amine functionalized) mesoporous silica catalysts were prepared by hydrothermal method. (3-[2-(2-amino ethyl amino) ethyl amino] propyl trimethoxysilane) and (3-mercaptopropyl) trimethoxysilane respectively were used as amine and sulfonic sources. The synthesised bifunctional materials were fully characterized by BET, P-XRD,  $^{29}\text{Si}$  CP/MAS-NMR, FTIR, XPS and SEM spectral analysis. FTIR and NMR results endorse the successful grafting of organic amines and sulfonic group by surface silanol of silica. The presence of N and S groups in the catalyst material was confirmed by the XPS spectra. Catalytic activity of the bifunctional material was tested for one-pot deacetalization–knoevenagel reaction, which gave excellent yield (95 %). Catalyst is reusable with little loss of activity up to 4 runs (<6 %).

**Keywords** Mesoporous silica · Sulfonic acid functionalization · Amine functionalization · One-pot reaction · Deacetalization–knoevenagel reaction

## 1 Introduction

For fine chemical synthesis, heterogeneous catalysts are preferred over the homogeneous ones due to the advantage of comparative ease of catalyst separation from the product streams which facilitate the design of persistent chemical processes [1]. Moreover, relative to their homogeneous analogues, heterogeneous catalysts are typically more acceptable

under extreme operating environments. Thus, heterogeneous solid acid and base catalysts offer more economic and eco-friendly processes relative to soluble acid and bases [2–6].

The stability and efficiency of catalysis relies on the choice of a suitable support material. In this regard over the period of time, various silicon-based supports such as  $\text{SiO}_2$ , mesoporous silica, silicon carbide have been developed [7]. Among these mesoporous silica based support materials, MCM-41 is considered ideal catalytic support, due to its high specific surface area ( $700\text{--}1,500\text{ m}^2\text{g}^{-1}$ ) as well as its uniform pore size (1.5–10 nm) [8]. Many researchers have attempted the mono functionalization of surface silanol group of MCM-41 with organic moieties. Such functionalization offers inorganic-organic hybrids, where the inorganic and organic ingredients are connected via strong interfaces contains covalent or ionic covalent bonds [9]. Literature survey shows that bifunctional hybrid materials have wider scope in the fields of catalysis [10–12], adsorption [13–18], sensor design [19] and nano science [20], but not much work is reported on the bifunctionalization of mesoporous silica [21–23].

Starting from the syntheses of small molecules to the elegant molecules, deacetalization through Knoevenagel condensation is well accepted norm in organic chemistry. It involves condensation of aldehydes with active methylene group compounds, and the reaction is both acid and base catalysed [24]. The condensation products, such as cinnamic acid, cinnamic and carboxylic functional derivatives are vital materials in flavour, perfumes and pharmaceuticals [25]. Of the various preparation methods possible, we employed lower acidic medium to protect the ( $-\text{NH}_2$ ) amine group. This approach is important to prevent the interaction between acid and base groups, which lead to the synthesis of novel bi-functional material. Hence, in this communication for the first time, we report an efficient protocol with good yields, for one-pot deacetalization–

S. Rana · S. Maddila · R. Pagadala · S. B. Jonnalagadda (✉)  
School of Chemistry and Physics, University of KwaZulu-Natal,  
Westville Campus, Chiltern Hills, Durban, KwaZulu-Natal 4000,  
South Africa  
e-mail: jonnalagaddas@ukzn.ac.za

Knoevenagel condensation reaction using novel bifunctional hybrid mesoporous material.

## 2 Experimental section

### 2.1 Synthesis of MCM-41

To a solution of 1.988 g of cetyl trimethylammonium bromide (CTAB, 98 %) in 120 g of H<sub>2</sub>O at room temperature, 8 ml of aqueous NH<sub>3</sub> was added, followed by 10 ml of tetraethyl orthosilicate (TEOS) (99 %) under continuous stirring (300 rpm). While the hydrolysis of TEOS takes place during the first 2 min (the solution becomes milky and slurry), the condensation of the mesostructured hybrid material was achieved after 1 h of reaction. The material was then filtered and allowed to dry under static air at 80 °C for 12 h. The surfactant removed mesoporous material was obtained by calcination at 550 °C for 5 h.

### 2.2 Preparation of final catalyst

1 g MCM-41 in 50 ml water was stirred for 30 min at room temperature, then 0.37 ml mercaptopropyl trimethoxysilane (MPTMS) and 0.84 mmol of silane(3-[2-(2-amino ethyl amino) ethyl amino] propyl trimethoxysilane) (AEPTMS) were added to the mixture. The mixture was heated in hydrothermal reactor for 6 h at 110 °C. The solution was

filtered and precipitate was dried 100 °C for overnight. The –SH group was oxidized to sulfonic acid, by heating 2.38 ml of 30 % H<sub>2</sub>O<sub>2</sub> in 7.14 ml methanol per 1 g of SH-AEPTMS@MCM-41 H<sub>2</sub>O<sub>2</sub> 50 °C for 24 h. The oxidized material was suspended in 25 ml of 1 wt% H<sub>2</sub>SO<sub>4</sub> for 4 h, washed with water, and then dried in vacuum (110 °C, 3 h). Again, the sample was mixed with aqueous solution of 0.01 M NaOH and stirred for 3 h. The product was repeatedly washed and filtered in de-ionised water until, the pH value of the filtrate is neutral. The final sample was designated as SO<sub>3</sub>H-AEPTMS@MCM-41.

### 2.3 Catalyst characterization

The surface area and pore size distribution of the catalysts were determined by N<sub>2</sub> adsorption–desorption at 77 K using ASAP 2020 (Micromeritics) instrument. Known amounts of the samples were evacuated for 2 h at 110 °C to remove physically adsorbed water prior to surface area measurements. The FT-IR spectra of the samples were recorded using Varian FTIR-800 in KBr matrix in the range of 4,000–400 cm<sup>-1</sup>. The PXRD patterns of the samples were obtained on Rigaku D/Max III VC diffractometer with Cu K $\alpha$  radiation at 40 kV and 40 mA in the range of 2 $\theta$  = 0–80°. The X-ray photoelectron spectra of various elements present were recorded using KRATOS apparatus with Mg, Al and Cu K $\alpha$  as X-ray sources. The samples for electron microscopy were prepared by

**Scheme 1** Schematic diagram of one-pot deacetalization–knoevenagel reaction

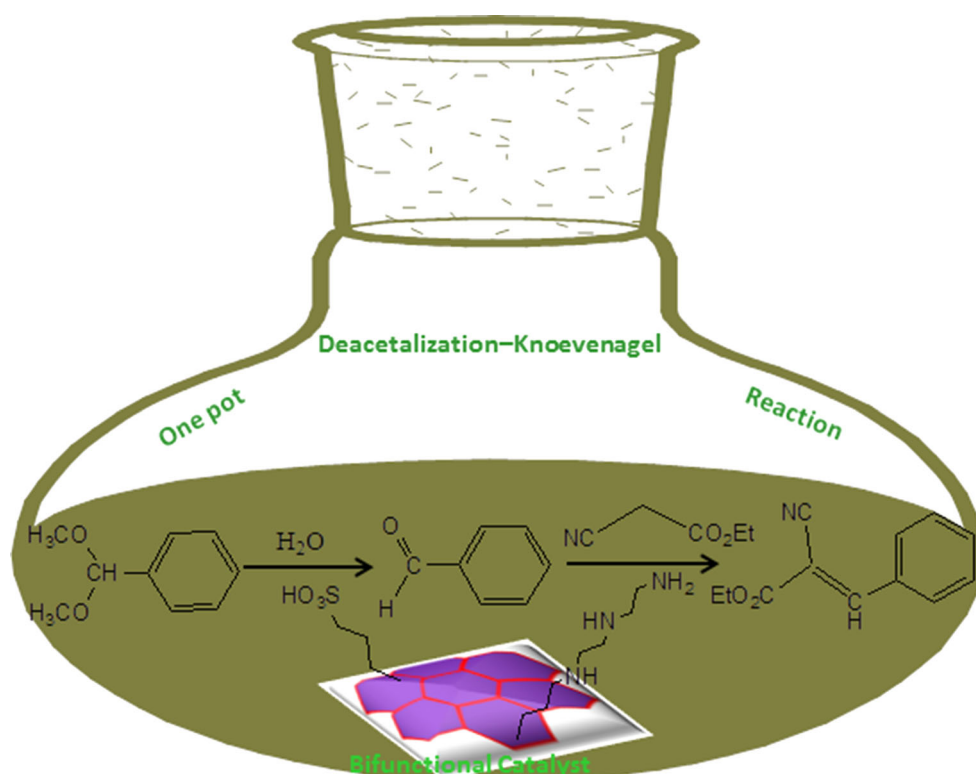


**Fig. 1** A, B FT-IR spectra of MCM-41 (a), SH-AEPTMS@MCM-41 (b) and SO<sub>3</sub>H-AEPTMS@MCM-41 (c)

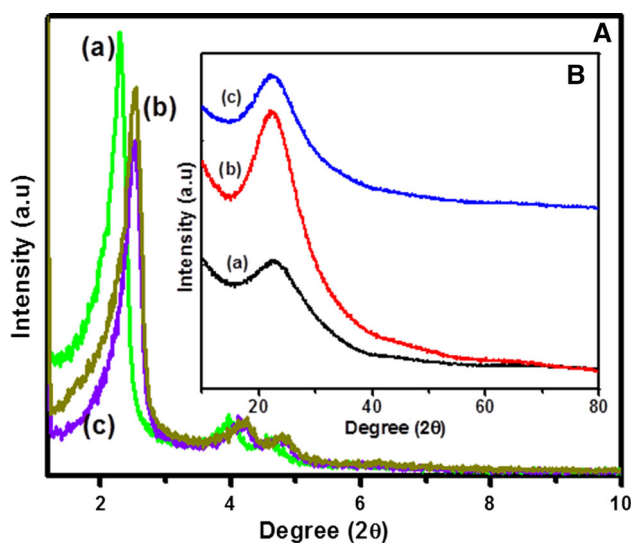
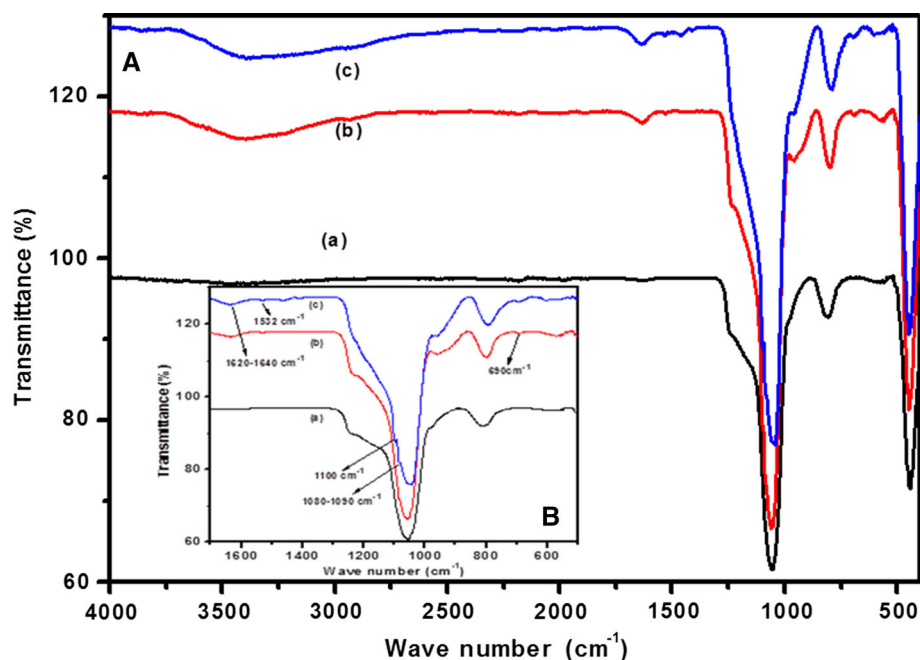


**Fig. 2** A, B SXAD & PXAD spectra of MCM-41 (a), SH-AEPTMS@MCM-41 (b) and SO<sub>3</sub>H-AEPTMS@MCM-41 (c)

dispersing the powder in ethanol and dropping a very dilute suspension on carbon coated Cu grids. The FE-SEM was performed with a ZEISS 55 microscope. Solid state <sup>29</sup>Si CP MAS NMR spectra were recorded on an AV300 NMR spectrometer.

### 3 General procedure for one-pot deacetalization–knoevenagel reaction

One-pot deacetalization-Knoevenagel reaction was carried out in a glass batch reactor fitted with a condenser. Catalyst

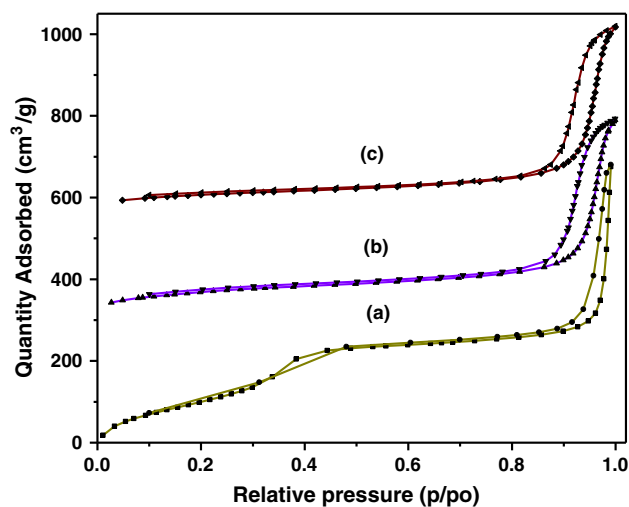


**Fig. 3** (a) N<sub>2</sub>-adsorption–desorption isotherm of MCM-41, (b) SH-AEPTMS@MCM-41 and (c) SO<sub>3</sub>H-AEPTMS@MCM-41

(0.15 g), H<sub>2</sub>O (12 ml), benzaldehyde dimethylacetal (4.0 mmol) and ethyl cyanoacetate (4.0 mmol) were taken in a 50 ml two necked round bottom flask. The mixture was vigorously stirred at 80 °C under nitrogen for 1 h as shown in Scheme 1. Then the catalyst was separated by filtration. The products were analyzed off-line by gas chromatography (Shimadzu GC-2010).

### 4 Results and discussion

The FT-IR spectra of acid–base modified sample and MCM-41 are shown in Fig. 1A, B. A perusal of the spectrum shows a

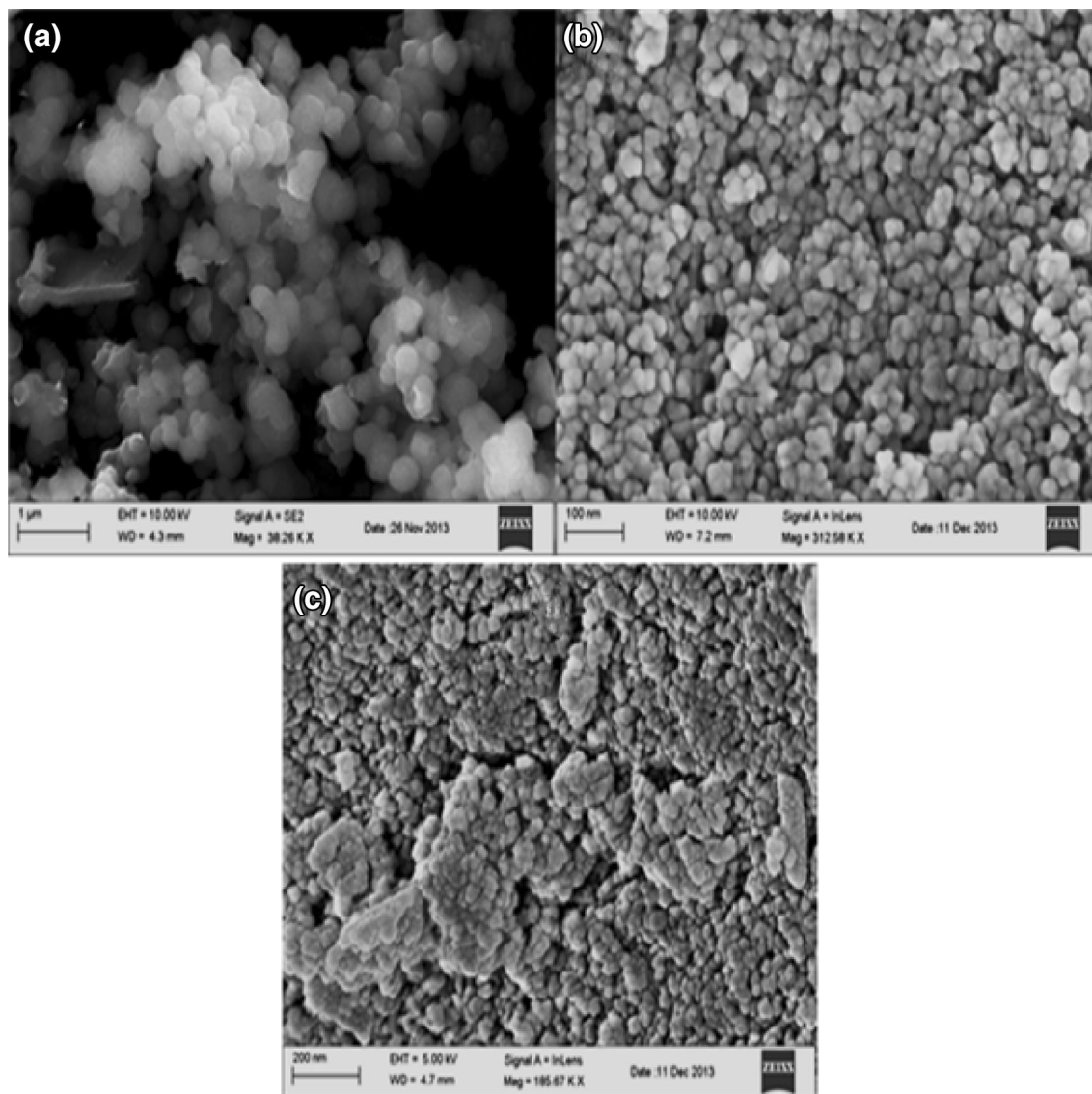
**Table 1** Surface properties of bifunctional catalyst

Catalyst	Surface area (m <sup>2</sup> g <sup>-1</sup> )	Pore volume (cm <sup>3</sup> g)
MCM-41	1,380	1.28
SH-AEPTMS@MCM-41	545	0.64
SO <sub>3</sub> H-AEPTMS@MCM-41	480	0.58

broad band of adsorbed water molecules around 3,100–3,600 cm<sup>-1</sup>. The characteristic absorption band at 1,620–1,640 cm<sup>-1</sup> is for H–O–H bending vibration in water [26]. The band, at 1,080–1,090 cm<sup>-1</sup> shows Si–O stretching in Si–O–Si structure [27]. The signal at 1,100 cm<sup>-1</sup> is due to S=O stretching vibration of sulfonic acid group. The existence of 690 cm<sup>-1</sup> for N–H bending vibration and 1,532 cm<sup>-1</sup> for –NH<sub>2</sub> symmetric bending vibration [27] in the synthesized

material and the absence of these two bending frequencies in parent MCM-41 sample, confirms the full grafting of organic amine covalently attached onto the support surface, i.e., amino group and sulfonic group are easily modified by surface silanol group of supported material.

The small angle XRD patterns of MCM-41, SH-AEPTMS@MCM-41 and SO<sub>3</sub>H-AEPTMS@MCM-41 are shown in Fig. 2A. All the three materials display a strong peak at  $2\theta = 2.2^\circ$  due to (100) plane and small peaks also indicate the formation of well-ordered mesoporous materials due to higher order (110), (200) and (210) plane reflections within 5°. Thus the mesoporosity remains unchanged after the modification of the silica network by both organo group and sulfonic acid. There is broadening and slight reduction of the (100) peak of SO<sub>3</sub>H-AEPTMS@MCM-41 after modification with both acid and base group on the support surface, suggest some

**Fig. 4** a SEM image of MCM-41, b SH-AEPTMS@MCM-41 and c SO<sub>3</sub>H-AEPTMS@MCM-41

marginal disturbance in hexagonal symmetry. The high angle XRD spectra of MCM-41, SH-AEPTMS@MCM-41 and SO<sub>3</sub>H-AEPTMS@MCM-41 are shown in Fig. 2B. An examination of the spectra in the Fig. 2B confirms that the materials did not basically change in structure as a result of functionalization i.e., the material remained intact after functionalization.

The N<sub>2</sub>-adsorption–desorption isotherm was carried for MCM-41, SH-AEPTMS@MCM-41 and SO<sub>3</sub>H-AEPTMS@MCM-41 are shown in Fig. 3. According to IUPAC nomenclature [28], the isotherm of the parent material shows a type IV isotherm. The initial increase in Nitrogen at low p/po was due to monolayer adsorption on the pore walls, and at intermediate p/po indicates the capillary condensation in the mesopores and higher p/po (plateau position) which is associated with the multilayer adsorption on the external surface of the materials. The BET surface area of parent MCM-41 sample was 1,380 m<sup>2</sup> g<sup>-1</sup>. The gradual decrease the surface area, and pore volume after loading of both acid and base (organo) groups are

summarised in the Table 1. This may be due to the presence of bulky materials inside the pores [29].

The Scanning electron microscopy of MCM-41 (a), SH-AEPTMS@MCM-41 (b) and SO<sub>3</sub>H-AEPTMS@MCM-41 (c) are shown in the Fig. 4. The parent material showed spherical morphology (Fig. 4a), but agglomerated spherical morphology was observed after modification of organic group. The change in morphology of the modified mesoporous materials might get influenced by the synthetic protocol of the materials.

EDX spectrum gives the information about the element present in the materials. Figure 5 shows EDX spectra of the MCM-41 (a), SH-AEPTMS@MCM-41 (b) and SO<sub>3</sub>H-AEPTMS@MCM-41 (c) samples, indicating the signals of the C, Si, N, and S elements present in the materials.

The total survey scan of acid–base bifunctional sample is shown in Fig. 6. This survey scan gives the information about the existence element like S, Si, O and N. The observed binding energies (Fig. 7) at 163.5 eV and 169.01 eV are for the S2p electron, which agree well with

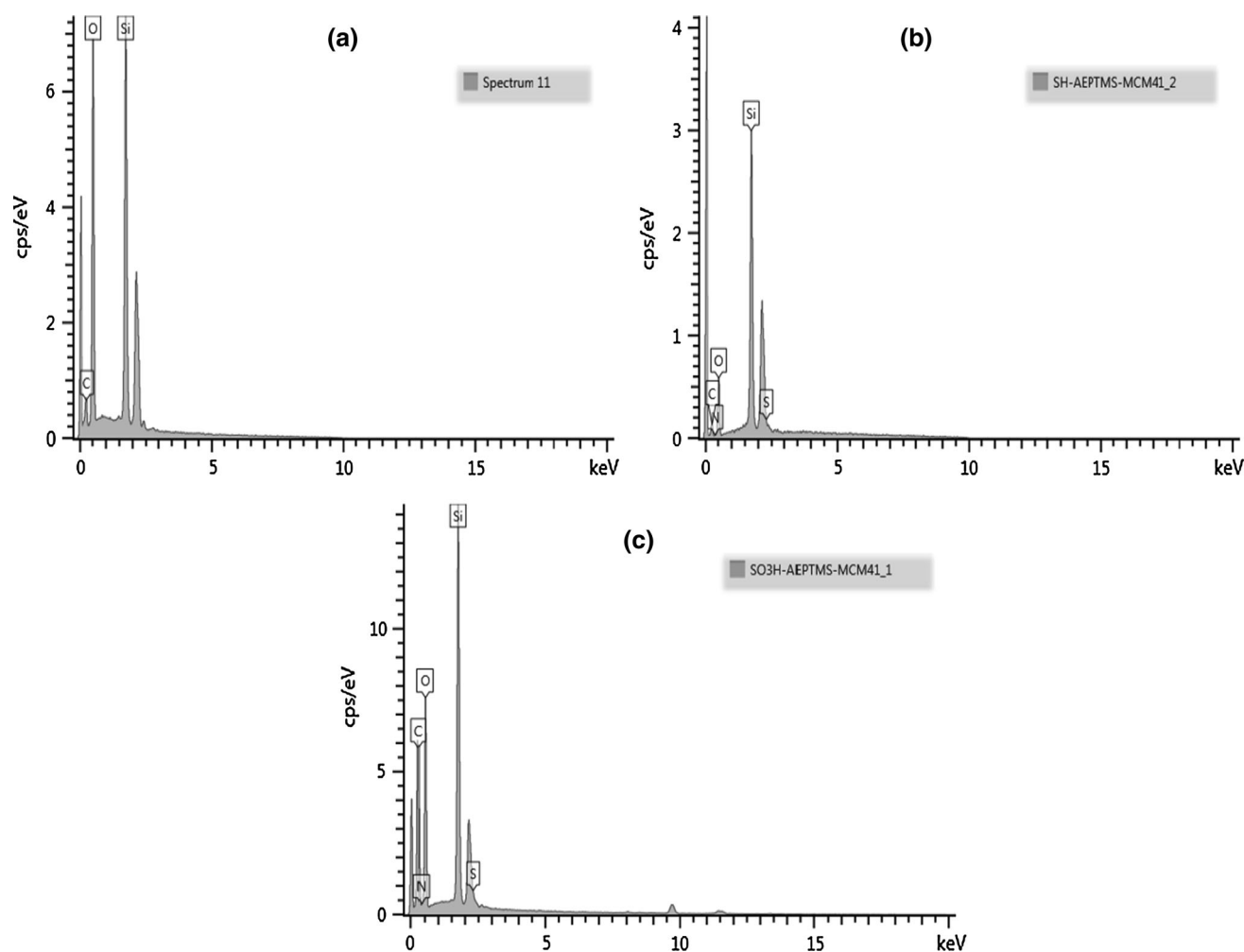


**Fig. 5** a EDX spectra of MCM-41, b SH-AEPTMS@MCM-41 and c SO<sub>3</sub>H-AEPTMS@MCM-41



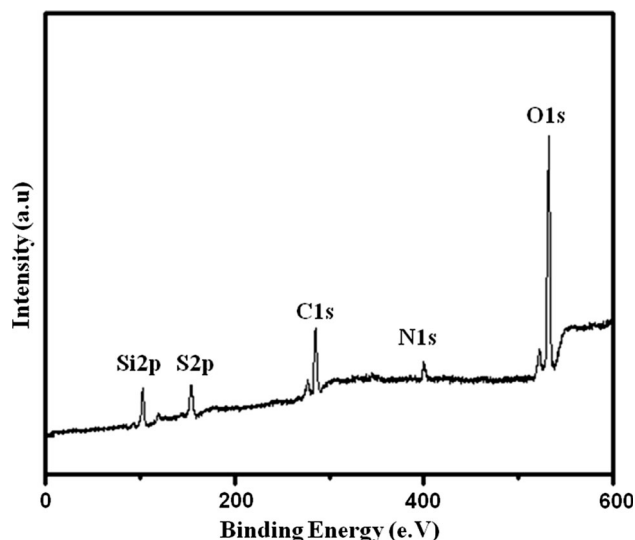


Fig. 6 Survey spectra of SO<sub>3</sub>H-AEPTMS@MCM-41 sample

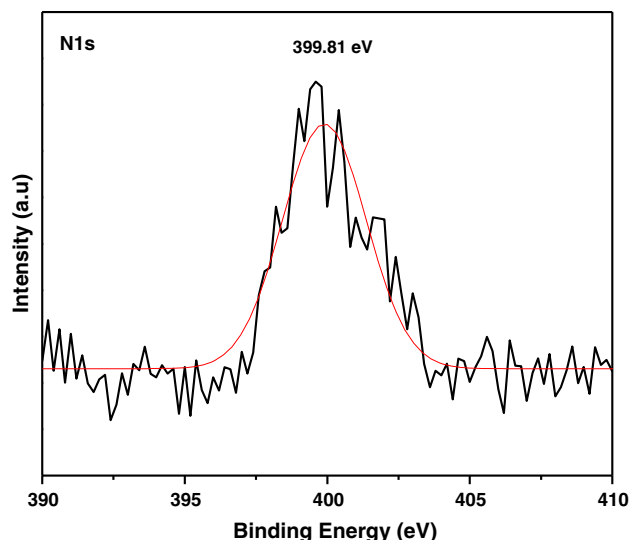


Fig. 8 XPS spectra of N1 s of SO<sub>3</sub>H-AEPTMS@MCM-41

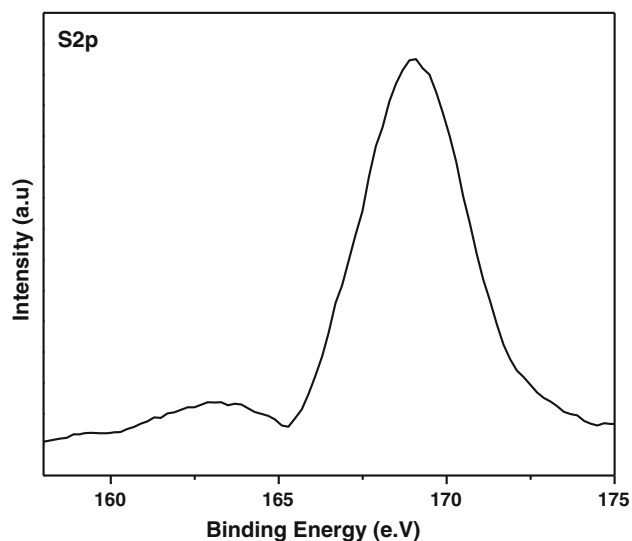


Fig. 7 XPS spectra of S2p of SO<sub>3</sub>H-AEPTMS@MCM-41catalyst

the literature reported the binding energies, 163 eV for the S2p electron of –SH group and binding energy of 169 eV for sulfonic acid group [30]. The observed results support that most of the –SH groups got successfully transformed to –SO<sub>3</sub>H by H<sub>2</sub>O<sub>2</sub>.

The standard binding energy for free amine group (–NH<sub>2</sub>) falls in the region of 399–401 eV, and protonated amine is 1.5 eV higher than the free amine group [31]. In our case, the N1s spectra of SO<sub>3</sub>H-AEPTMS@MCM-41 showed peak at 399.81 eV (Fig. 8). During the preparation although there is some scope for protonation of some –NH<sub>2</sub> groups by acid, they get deprotonated due to the presence of strong base. The XPS spectra confirms that, organic amino group were successfully grafted by surface silanol group of mesoporous material.

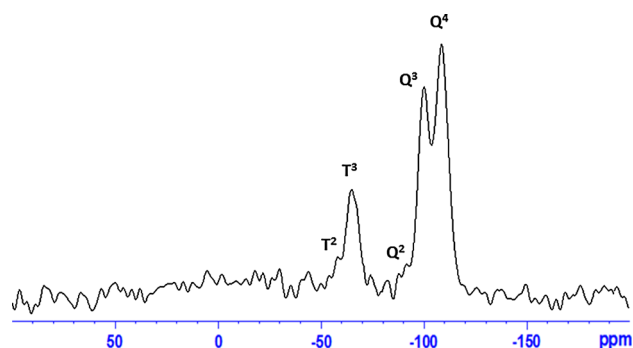


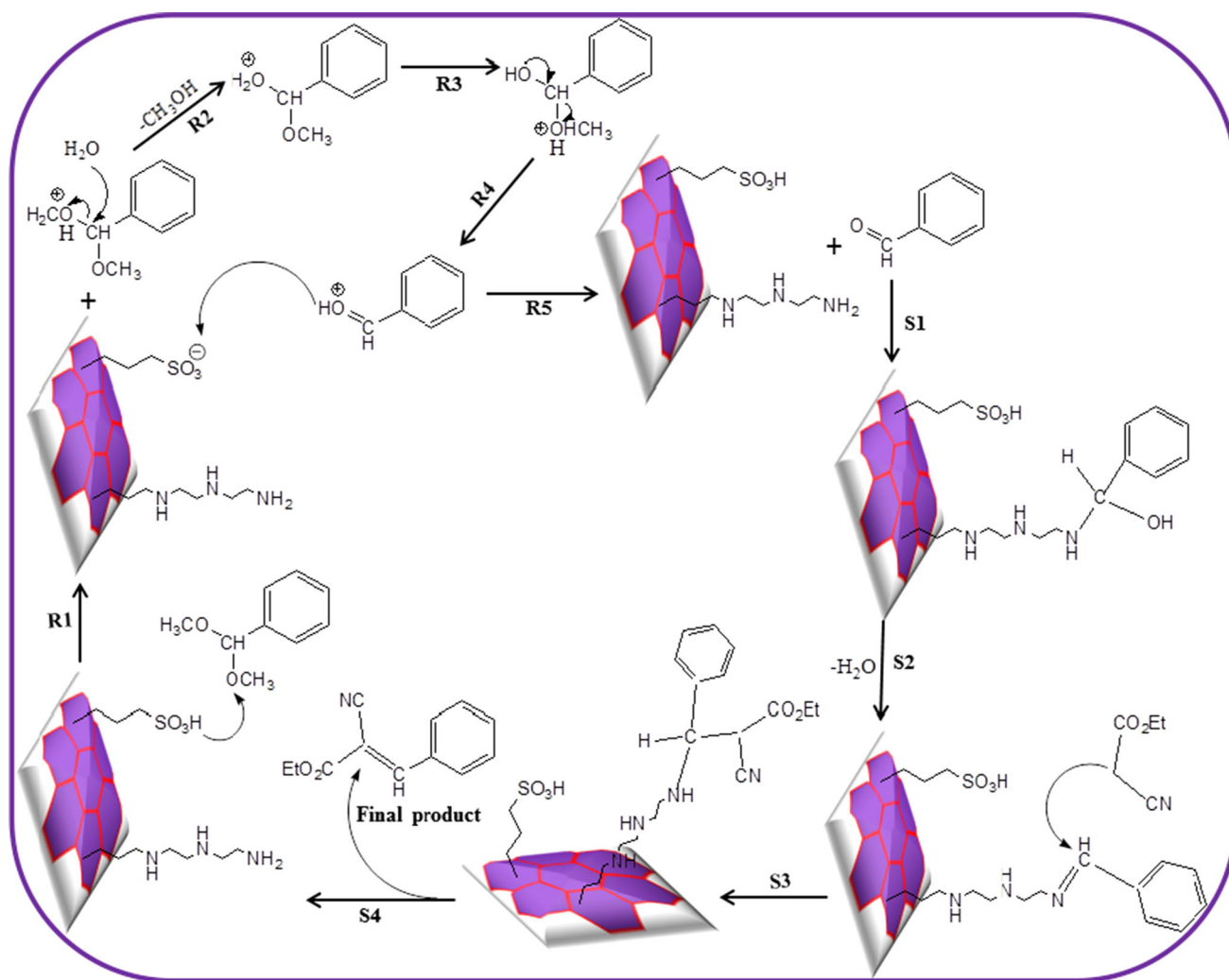
Fig. 9 <sup>29</sup>Si CPMAS NMR spectra of SO<sub>3</sub>H-AEPTMS@MCM-41

<sup>29</sup>Si CPMAS NMR spectrum of SO<sub>3</sub>H-AEPTMS@MCM-41 material is shown in Fig. 9. The three peaks at –111.02, –101.75 and –92 ppm in the NMR spectrum correspond to siloxane species of Q bands; and other two peaks at –66.71 and –57.84 ppm represent T<sup>3</sup> and T<sup>2</sup> bands respectively. Thus, the spectrum confirms the successful covalent grafting of functional group through the Si–O–M linkage.

The SO<sub>3</sub>H-AEPTMS@MCM-41 with acid and base groups has potential to accelerate both acid and base catalyzed reactions and is ideal of one-pot reaction setup. Shang et al. [32] reported the use of acid–base bifunctional mesoporous silica for deacetalization–Knoevenagel reaction. While they used mono amine (APTES) for basic sites, we incorporated a triamine [silane(3-[2-(2-amino ethyl amino) ethyl amino] propyl trimethoxysilane (AEPTMS))] for basic sites in the catalyst. The triamine functionalized materials more basic relative to mono amine functionalized ones. The scope of SO<sub>3</sub>H-AEPTMS@MCM-41 as catalyst for one-pot deacetalization–Knoevenagel reaction was explored. A perusal of the results summarised in Table 2 shows that reaction was well

**Table 2** One-pot deacetalization–knoevenagel reaction over all catalysts

Catalyst	Conversion % (1)	Yield (2)	Yield (3)
MCM-41	Trace	Trace	Trace
AEPTMS@MCM-41	Trace	Trace	Trace
SO <sub>3</sub> H@MCM-41	58.65	55.34	0
SO <sub>3</sub> H-AEPTMS@MCM-41	100	5.1	94.9
SO <sub>3</sub> H-AEPTMS@MCM-41 (1st cycle)	100	5.0	95
SO <sub>3</sub> H-AEPTMS@MCM-41 (2nd cycle)	99.89	5.1	94.9
SO <sub>3</sub> H-AEPTMS@MCM-41 (3rd cycle)	99.95	5.3	94.7
SO <sub>3</sub> H-AEPTMS@MCM-41 (4th cycle)	94	10.7	89.3



**Scheme 2** Proposed mechanism of one-pot deacetalization–knoevenagel reaction

completed in 1 h at 80 °C giving 95 % yield than other MCM-41, AEPTMS@MCM-41 and SO<sub>3</sub>H@MCM-41 catalysts.

The reaction mechanism of one-pot process on the catalyst surface may be expressed as follows: First step is initiated by

acidic site, which followed by the basic site catalysed reaction to give the condensed product (Scheme 2). From R1 to R5 intermediate states, the conversion of benzaldehyde dimethyl acetal to benzaldehyde by acid catalyst is shown. In

the second step, the  $-NH_2$  group goes through nucleophilic attack on the carbonyl carbon (S1) and in the consequent step water is released resulting in formation of imine intermediate (S2). In the last step, ethyl cyanoacetate reacts with the intermediate (S3), finally resulting in formation of ethyl cyanocinnamate and restoring of amine (S4).

The scope of recycle of the catalyst was examined by carrying out repeated reactions using the recovered catalyst. After the reaction, the catalyst was separated by centrifugation, washed with distilled water in several times, again dried and reused in the reaction with afresh reaction mixture. The yield decreased by 5.7 % in the regenerated sample in the 4th cycle, which suggests that covalently attached bifunctional groups were stable and robust, allowing the recycle and reuse of catalyst for without significant loss of activity.

## 5 Conclusions

The acid–base bifunctionalized mesoporous silica was successfully synthesised through a simple hydrothermal method. Successful grafting of acid and base group by surface silanol group of mesoporous silica was confirmed by FTIR and NMR spectra. The bifunctional catalyst gave excellent yield (95 %) of products in one-pot deacetalization–Knoevenagel reaction with short reaction time. The regeneration/reusability test shows the good recycling capacity of the functionalized material.

**Acknowledgments** The authors are grateful to the School of Chemistry & Physics and the College of Agriculture, Engineering & Science, University of KwaZulu-Natal, Westville campus, Durban, South Africa for the facilities and financial support.

## References

1. M. E. Davis, R. J. Davis, (ISBN, New York, ISBN 0-07-245007-X, 2003) **133**
2. K.R. Kloetstra, V. Bekkum, J. Chem. Soc. Chem. Commun. **10**, 1005–1006 (1995)
3. Y.V. SubbaRao, D.E. De Vos, P.A. Jacobs, Angew. Chem. Int. Ed. Engl. **36**, 2661 (1997)
4. K. KoteswaraRao, M. Gravelle, J. Sanchez, F. Figueras, J. Catal. **173**, 115 (1998)
5. F. Cavani, F. Trifiro, A. Vaccari, Catal. Today **11**, 173 (1991)
6. M. Lakshmi Kantam, B. M. Choudary, C.Venkat Reddy, K. KoteswaraRao, F. Figueras, J. Chem. Soc. Chem. Commun. 1033 (1998)
7. N. Keller, R. Vieira, J.M. Nhut, C. Pham-Huu, M.J. Ledoux, J. Braz. Chem. Soc. **16**(2), 202 (2005)
8. Y. Ren, B. Yue, M. Gu, H. He, Materials **3**, 764 (2010)
9. C. Sanchez, B. Julián, P. Belleville, M. Popall, J. Mater. Chem. **15**, 3559 (2005)
10. A. Stein, Adv. Mater. **15**, 763 (2003)
11. I.K. Mbaraka, D.R. Radu, V.S.-Y. Lin, J. Catal. **219**, 329 (2003)
12. X.G. Wang, C.-C. Chen, S.-Y. Chen, Y. Mou, S. Cheng, Appl. Catal. A. Gen. **281**, 47 (2005)
13. K.Y. Ho, G. McKay, K.L. Yeung, Langmuir **19**, 3019 (2002)
14. T. Yamamoto, T. Tanaka, T. Funabiki, S. Yoshida, J. Phys. Chem. B **102**, 5830 (1998)
15. X. Feng, G.E. Fryxell, L.Q. Wang, A.Y. Kim, J. Liu, K.M. Kemner, Science **276**, 923 (1997)
16. L. Mercier, T.J. Pinnavaia, Environ. Sci. Technol. **32**, 2749 (1998)
17. R.I. Nooney, M. Kalyanaraman, G. Kennedy, E.J. Maginn, Langmuir **17**, 528 (2001)
18. J.F. Diaz, K.J. Balkus, F. Bedioui, V. Kurshev, L. Kevan, Chem. Mater. **9**, 61 (1997)
19. V.S.-Y. Lin, C.-Y. Lai, J. Huang, S.-A. Song, S. Xu, J. Am. Chem. Soc. **123**, 11510 (2001)
20. W.H. Zhang, X.B. Lu, J.H. Xiu, Z.L. Hua, L.X. Zhang, M. Robertson, J.L. Shi, D.S. Yan, J.D. Holmes, Adv. Funct. Mater. **14**(6), 544 (2004)
21. L.Y. Shi, Y.M. Wang, A. Ji, L. Gao, Y. Wang, J. Mater. Chem. **15**, 1392 (2005)
22. P. Li, X. Zhang, Y.J. Chen, T.Y. Bai, H.Z. Lian, X. Hu, RSC. Adv **4**, 49421 (2014)
23. W. Xu, Q. Gao, Y. Xu, D. Wu, Y. Sun, W. Shen, F. Deng, J. Solid State Chem. **181**(10), 2837 (2008)
24. Y. Peng, J. Wang, J. Long, G. Liu, Catal. commu **15**(1), 10 (2011)
25. A.K. Sinha, N. Sharma, A. Shard, A. Sharma, R. Kumar, U.K. Sharma, Indian J. Chem. 1771 (2009)
26. B.J. Saikia, G.K. Parthasarathy, J. Mod. Phys **1**, 206 (2010)
27. K.M. Parida, D. Rath, J. Mol. Catal. A: Chem. **310**, 93 (2009)
28. S. Brunauer, L.S. Deming, E. Deming, E. Teller, J. Am. Chem. Soc. **62**, 1723 (1940)
29. H. Yang, G. Zhang, X. Hong, Y. Zhu, J. Mol. Cat. A **210**, 143 (2004)
30. H. Moulder, W. F. Stickle, P. E. Sobol, K. D. Bomden, X-ray photoelectron Spectrosc. J. Chast. (1992)
31. L. Zhang, J. Liu, J. Yang, Q. Yang, C. Li, Microporous Mesoporous Mater. **109**, 172 (2008)
32. F. Shang, J. Sun, S. Wu, Y. Yang, Q. Kan, J. Guan, Microporous Mesoporous Mater. **134**, 44 (2010)